

## Free-running performance and full control of a passively phase-stable Er: fiber frequency comb

D. FEHRENBACHER, P. SULZER, A. LIEHL, T. KÄLBERER, C. RIEK, D. V. SELETSKIY, AND A. LEITENSTORFER\*

Department of Physics and Center for Applied Photonics, University of Konstanz, D-78457 Konstanz, Germany

\*Corresponding author: [Alfred.Leitenstorfer@uni-konstanz.de](mailto:Alfred.Leitenstorfer@uni-konstanz.de)

Received 23 July 2015; revised 12 September 2015; accepted 22 September 2015 (Doc. ID 246497); published 20 October 2015

Optical frequency combs based on erbium-doped fiber lasers are attractive tools in precision metrology due to their inherent compactness and stability. Here we study a femtosecond Er: fiber comb that passively eliminates the carrier-envelope phase slip by difference frequency generation. Quantum statistics inside the all-fiber soliton oscillator governs its free-running performance. Active stabilization of the repetition rate supports a subhertz optical linewidth and does not necessitate additional intracavity elements. Direct locking to an optical atomic frequency standard enables generation of a 100 MHz microwave signal with a stability of 3.4 mHz maintained over 15 min. © 2015 Optical Society of America

**OCIS codes:** (120.3940) Metrology; (140.4050) Mode-locked lasers; (320.7100) Ultrafast measurements; (130.7405) Wavelength conversion devices.

<http://dx.doi.org/10.1364/OPTICA.2.000917>

### 1. INTRODUCTION

Years after the first demonstration of high-resolution spectroscopy in the frequency domain with femtosecond lasers [1,2], the number of applications of frequency combs in precision metrology is ever growing [3]. Recently, a relative precision of  $10^{-18}$  was reached using the transfer oscillator concept [4]. Currently, one of the main goals of research is focused on finding new implementations for long-term stable, precise, and robust comb sources [5]. Realizations based on fiber lasers are especially known for extraordinarily long-term stability due to nearly monolithic design with minimal free-space components. The appeal of this technology as the tool of choice for hands-off operation has grown rapidly since the first demonstration of self-referencing [6,7] and active frequency locking [8]. Recent progress is based on all-fiber implementations of  $f$ -to- $2f$  interferometry and feedback loops exploiting fast intracavity actuators [9,10]. This approach supports polarization-maintaining fiber oscillators mode locked by saturable absorbers. A different scheme has been demonstrated for solid-state lasers via frequency stabilization with an acousto-optic modulator outside the cavity [11]. The advantage of extracavity active elements is that they do not compromise oscillator performance: the feedback-induced cross talk between the orthogonal variables of the comb, namely, the repetition rate ( $f_{\text{rep}}$ ) and the carrier-envelope offset (CEO) frequency ( $f_{\text{CEO}}$ ), is virtually absent. A completely passive approach is to eliminate the CEO frequency via extracavity difference frequency generation (DFG) between spectral components of the amplified and frequency-broadened oscillator [12]. In this case, optical feedback is based on an ultrafast nonlinearity, which provides maximal bandwidth at the full repetition rate of the pulse train. No

electronic control loop utilizing an RF source is therefore needed, dramatically reducing the complexity and enhancing the quality of the long-term performance. Recently, we demonstrated a passively phase-locked Er: fiber system with amplified DFG at the fundamental wavelength of 1550 nm and quantified its carrier-envelope-phase (CEP) stability [13]. Ultrabroad spectral components required for the DFG are achieved from dispersion-managed highly nonlinear germanosilicate fibers [14]. A phase-stable pulse train spanning from 136 THz (2200 nm) to 370 THz (810 nm) can be generated with this approach. Tuning the output of the DFG to the Er: fiber gain window allows for reamplification via standard telecom components, providing an intense and fully coherent output of phase-stable pulses [15,16]. Inherent stability of the CEP is especially appealing for space-based applications [17,18] and high-power fiber systems aiming at sensitive experiments in extreme nonlinear optics [19]. Very recently, a DFG comb from an Yb: fiber oscillator mode locked via nonlinear polarization rotation was stabilized to a linewidth of 1 kHz by coupling to an external reference cavity [20].

In this work, we present a compact and passively phase-stable Er: fiber frequency comb. The self-starting all-fiber oscillator is mode locked by a semiconductor saturable absorber. Together with a fully polarization-maintaining design, these characteristics enable excellent long-term performance and reliability. Detailed analysis of the free-running system reveals quantum-limited operation. The comb is stabilized without introducing additional intracavity elements. A subhertz linewidth is achieved via locking to an external single-frequency laser. A microwave signal with fractional stability of  $3.4 \times 10^{-11}$  over a 15 min time span results from direct referencing to a two-photon transition in  $^{85}\text{Rb}$ .

## 2. EXPERIMENTAL SETUP AND CHARACTERIZATION

The layout of the system is presented in Fig. 1. The master oscillator is a robust Er: fiber laser consisting only of polarization-maintaining (pm) components with no free-space parts. Self-starting and stable mode locking is granted by a pigtailed saturable absorber mirror. This oscillator emits up to 5 mW of average power at a repetition rate of 100 MHz and a center frequency of 193 THz (1556 nm). Overall negative intracavity dispersion of  $-12000 \text{ fs}^2$  supports a train of soliton pulses with a bandwidth tunable between 12 and 18 nm via the current of the pump diode. The average power is boosted to 600 mW by means of a single-pass amplifier relying completely on polarization-maintaining fiber. Controlled self-phase modulation is used to broaden the seed spectrum to a width of 60 nm, enabling the temporal compression of the pulses to a duration of 120 fs via a silicon prism sequence. The amplified pulse train is coupled into a dispersion-managed highly nonlinear germanosilicate fiber 1 cm in length [13], resulting in an ultrabroad spectrum spanning from the soliton at 136 THz (2200 nm) to the dispersive wave covering up to 370 THz (810 nm), with 35 mW and up to 80 mW of average power, respectively. The soliton pulse propagates in a region of anomalous dispersion and leaves the highly nonlinear fiber (HNF) already bandwidth-limited, whereas the dispersive wave requires dispersion management. A special arrangement is implemented to simultaneously compress the dispersive wave and set the relative timing between the two pulses (see Fig. 1). It maximizes the common path between both spectral components by

sharing all but two optical elements. This implementation enables outstanding long-term stability in comparison to a conventional Mach-Zehnder geometry. The output of the HNF is spatially dispersed by the first SF10 prism, and wavelengths above  $1.3 \mu\text{m}$ , containing fundamental and soliton spectral components, are directed onto a spherical end mirror (SM2,  $f = 7.5 \text{ cm}$ ). The prism tip is located exactly at the distance equal to the radius of curvature of this mirror, thus ensuring reversal of spatial dispersion of the spectral components. Residual pump at 1550 nm with  $f_{\text{CEO}} \neq 0$  is blocked by a razor blade placed before SM2. Our design ensures that the soliton pulse duration of 30 fs is unaffected due to the proximity of the pulse center frequency to the zero-crossing of the group velocity dispersion in SF10 at 1710 nm. Instead, the dispersive wave is compressed to 25 fs upon double passage through the prism sequence. The collimated dispersive wave is spatiotemporally overlapped with the soliton on a spherical mirror (SM1,  $f = 20 \text{ cm}$ ). Subsequently, both components are focused (SM3,  $f = 2.5 \text{ cm}$ ) into a 2 mm long lithium niobate crystal with a fan-out poling period ranging from 21 to 35  $\mu\text{m}$ . The phase-stable output with 500  $\mu\text{W}$  of average power is generated via difference frequency mixing and coupled back into a fiber for amplification to 2.5 mW. The pulse train is then split in two parallel branches. One is amplified to an average power of 630 mW, which is, to the best of our knowledge, the highest power yet reported for a single-mode-pumped fs Er: fiber laser. Subsequently, the output pulses are compressed to a duration of 110 fs with the target of direct locking to a rubidium vapor cell. The other branch is used for beat experiments and locking of selected comb lines to single-line lasers.

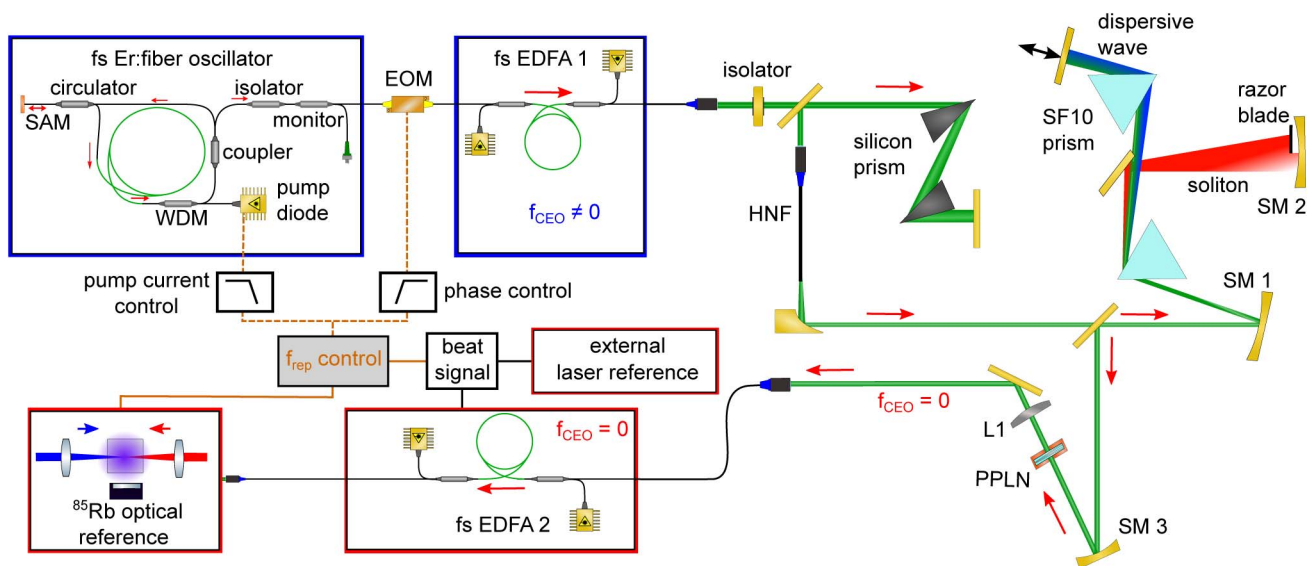


**Fig. 1.** Schematic of the phase-stable Er: fiber system. An optical pulse train at a 100 MHz repetition rate is generated in an all-fiber oscillator (SAM, saturable absorber mirror; WDM, wavelength division multiplexer) and amplified in a polarization-maintaining Er: fiber amplifier (fs EDFA 1). It enters a free-space section (right) where it is first compressed by a silicon prism sequence and then frequency broadened in a dispersion-managed highly nonlinear fiber (HNF) to a coherent supercontinuum spanning more than one octave. Compactness and stability are optimized by a special SF10 prism compressor that simultaneously controls short pulse duration and temporal overlap between a dispersive wave and the solitonic part of the continuum. A razor blade removes residual pump light at 1550 nm. Difference frequency mixing in a periodically poled lithium niobate crystal (PPLN; length = 2 mm) results in a frequency comb without carrier-envelope offset (CEO). Active linewidth narrowing is accomplished by locking the beat signal between the amplified phase-stable comb and a single-frequency laser at 193 THz to a radio frequency. The pump current is exploited as an actuator to control the feedback signal at low frequencies. An extracavity electro-optic modulator (EOM) eliminates residual phase jitter at high frequencies. Absolute stability of the system is ensured by locking the repetition rate of the offset-free comb to an atomic two-photon transition in a  $^{85}\text{Rb}$  cell. Orange lines depict electronic connections carrying error (solid) and feedback (dashed) signals used in active stabilization loops. The setup contains spherical mirrors SM1, SM2, and SM3 with focal lengths of 20, 7.5, and 2.5 cm, respectively, and a collimating lens L1 with  $f = 1.8 \text{ cm}$ .

### 3. BROADBAND STUDY OF THE COMB LINEWIDTH

To investigate the linewidth of our phase-stable comb, we perform beat measurements with various narrow-linewidth sources. First, we employ an Er:fiber single-line laser operating at 193 THz (1556 nm) with a spectral bandwidth of less than 2.5 kHz over 1 ms of observation time. The pulse train is mixed with the single-line laser in a fiber coupler. After passing a bandpass filter with a bandwidth of 0.5 nm, both are overlapped on a pigtailed InGaAs photodiode. The beat between the single-frequency laser and the Er:fiber oscillator reveals a reference-limited linewidth below 10 kHz at an observation time of 12 ms when recorded with an RF spectrum analyzer. The linewidth of the phase-stable frequency comb is instead determined to be  $91 \pm 6$  kHz at a wavelength of 1556 nm [inset of Fig. 2(a)]. While this performance is already attractive for a CEO-stabilized all-fiber laser system [9,21], it also raises the question of the mechanism of the increase in the linewidth observed in comparison to the oscillator performance. To uncover the origin of this broadening, a full understanding of the spectral distribution of the linewidth in the supercontinuum output of the HNF is mandatory. For this purpose, we use an additional single-line laser (Nd:YAG emitting at 282 THz with a linewidth of 1 kHz over an observation time of 100 ms) to characterize the dispersive as well as the solitonic part of the spectrum. Beat experiments on the ultrabroad spectrum generating the phase-stable pulse train are summarized in Fig. 2(a). The spectral width of the oscillator at 1556 nm is determined to be below 10 kHz, largely limited by the performance of the single-line laser. In contrast, the linewidth increases to  $25 \pm 4$  kHz at a wavelength of 1064 nm. In addition, a  $30 \pm 4$  kHz linewidth is revealed by the beat note between the frequency-doubled soliton at 2128 nm (141 THz) and the Nd:YAG reference. To further investigate this context, we study the RF noise spectrum  $S_v(f)$  of our system [Fig. 2(b)]. To this end, an adequately sampled time series of 400 ms of the beat signal is recorded with an oscilloscope. This allows for phase retrieval with a modified Takeda algorithm [22]. The obtained noise spectrum of the beat note between the oscillator (blue line) and the single-line laser (green line, manufacturer data) is reference-limited. The RF spectrum of the DFG output at 1550 nm is depicted as a red

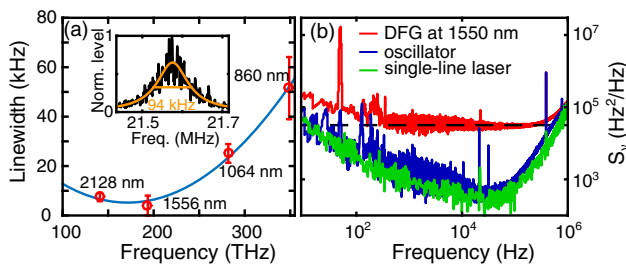


**Fig. 2.** (a) Measured linewidth (open circles) and parabolic fit (blue line) versus optical frequency of the supercontinuum output from the highly nonlinear fiber. Inset: Characteristic beat note of the phase-stable comb with a single-line reference at 1556 nm recorded at a resolution bandwidth of 1 kHz at 12 ms sweep time. (b) Frequency noise spectra of the reference with the oscillator (blue) and the phase-stable comb (red) in comparison to the reference performance (green, data from manufacturer). Note the characteristic flat spectrum of the comb, indicating white frequency noise (see dashed line). A small deviation above 300 kHz is explained by the performance of the reference.

line in Fig. 2(b). The white frequency noise found over a broad range from 200 Hz up to 300 kHz suggests that the origin of the linewidth is due to the quantum statistics of the laser emission [23]. Analysis of the phase noise [24] indicates a linewidth of the comb at 2128 nm of  $8 \pm 2$  kHz. Further insight may be gained from careful inspection of the origin of the 91 kHz linewidth of the phase-stable comb at 1556 nm. This value results from nonlinear mixing between the comb lines at 860 and 1950 nm. Anticorrelated changes in the linewidth of these components are expected for a breathing motion of the comb about its center frequency [25], as it results from the timing jitter of the repetition rate in agreement with our measurements. Without taking into account the technical noise contributions below 200 Hz, the linewidth at 860 nm is given by  $\delta\nu_{\text{disp}} = \delta\nu_{\text{sol}} + \delta\nu_{\text{DFG}} - 2\sqrt{\delta\nu_{\text{sol}}\delta\nu_{\text{DFG}}}$ . From this, the linewidth of the 860 nm component is determined to be  $52 \pm 13$  kHz. The combined measurements reveal a quadratic increase in the linewidth of the comb away from the vertex close to the carrier frequency [Fig. 2(a)]. This finding indicates that the comb performance is dominated by the Gordon–Haus jitter [26] of the oscillator originating from the amplitude-to-phase conversion of the shot noise. It is consistent with the fact that fluctuations of the average photon number at the output of an ideal solitonically mode-locked laser should be governed by quantum statistics [27].

Next, we alter the pulse energy circulating in the oscillator by changing the pump current. Emitting clearly soliton-shaped spectra [inset of Fig. 3(b)], the FWHM varies from 12 to 18 nm when the pump current ( $I_p$ ) is increased from 370 to 880 mA [Fig. 3(a)]. These changes in the bandwidth should have profound effects on the linewidth if the performance of the oscillator is quantum-limited [28]. Therefore, the linewidth of the phase-stable comb is monitored together with the linewidth of the comb lines at 1064 and 2128 nm. Upon increasing the pump current, we observe pronounced narrowing of the optical linewidth by a factor of 3, commensurate with the increase in the bandwidth [Fig. 3(a)]. This behavior is drastically reversed upon reaching a pump current of 730 mA, and already at 850 mA the linewidth exceeds the value at the mode-locking threshold. The optimal linewidth occurs at the point of balance between the quantum-limited reduction of the Gordon–Haus jitter and the eventual

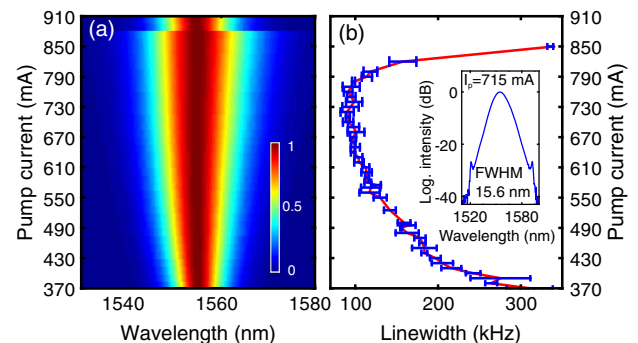


**Fig. 3.** (a) Output spectrum of the oscillator for pump currents from 370 to 910 mA. Due to the soliton condition, the bandwidth increases from 12 to 18 nm with an increase in the pump current. (b) Decrease in the linewidth of the phase-stable pulse train at a wavelength of 1550 nm with an increase in the pump current due to the commensurate reduction in Gordon–Haus jitter. Inset: Output spectrum of the oscillator at a pump current ( $I_p$ ) of 715 mA highlights an excellent  $\text{sech}^2$  shape (note the logarithmic ordinate scale).

onset of soliton fission due to the high circulating peak power inside the laser cavity. To exclude the intensity noise of the pump diode as a potential origin of this behavior [29], the linewidth measurements are repeated at the same nominal pump powers but with changed relative intensity noise (RIN) levels. This is accomplished by insertion of a fiber coupler between the pump diode and the WDM (Fig. 1), allowing for constant optical output with drastically changed pump current. We observe negligible influence on the linewidth when the outlined changes in the pump current and RIN levels of our excitation diode laser are implemented. We emphasize that the quadratic linewidth dependence away from the center frequency of the comb [Fig. 2(a)], the white frequency noise spectrum of the comb beat [Fig. 2(b)], and the decrease in the linewidth with the increasing spectral bandwidth of the oscillator (Fig. 3) provide independent verifications for the quantum origin of the noise of our oscillator.

#### 4. ACTIVE LINewidth NARROWING

For a variety of applications not only a fixed CEO frequency but also a narrow optical linewidth is mandatory, supporting, for example, subhertz precision in optical spectroscopy [30] or low-noise RF frequency standards [31,32]. In addition to fixing  $f_{\text{CEO}}$  of the comb, the repetition rate has to be stabilized. Traditionally, the CEO frequency in fiber-based oscillators is controlled by changing the refractive index of the gain medium with the pump power. The repetition rate is influenced by the variation in the length of the laser cavity, altered, e.g., by a mirror placed on a piezo actuator or a fiber stretcher. Additional actuators such as electro-optic modulators (EOMs) may be inserted in the oscillator to achieve maximum bandwidth. However, all these control elements exhibit considerable cross talk when operating jointly inside the all-fiber cavity, rendering electronic control of the comb tedious. Furthermore, any additional intracavity active components would be detrimental for quantum-limited operation of the laser, potentially spoiling the high-quality performance of our solitonic oscillator [27]. The fact that only the repetition rate has to be controlled in our  $f_{\text{CEO}} = 0$  comb allows us to elegantly circumvent those issues. We can completely control  $f_{\text{rep}}$  without adding any extra components to the mode-locked laser oscillator. Influencing the intracavity power by changing the current of the pump diode from 500 to 750 mA allows us to correct the repetition rate by as much as 100 Hz with a modulation bandwidth of 70 kHz when employing a phase lead technique [29]. Additional bandwidth can be provided by an extracavity electro-optic phase shifter [33]. In our comb, high-frequency phase noise is present due to the quantum origin of its free-running performance. Fortunately, very little dynamic range is required to carry out phase correction with a fiber-coupled EOM inserted between the oscillator and the amplifier (Fig. 1). To demonstrate the capabilities of our stabilization scheme, we first achieve active locking and optical linewidth narrowing using a Rb-stabilized RF waveform synthesizer. A beat note between the amplified phase-stable comb and a single-line reference at 1556 nm is generated and locked onto a fixed RF reference. The power of the relevant comb mode is 30 nW, and the RF beat signal exhibits a signal-to-noise ratio of 35 dB when detected with a resolution bandwidth (RBW) of 1 kHz. It is split into two parts. One branch provides feedback for two proportional–integral–derivative (PID) controllers, and the other portion is used for analysis of the RF spectrum, frequency noise, and phase jitter of the beat note. The performance

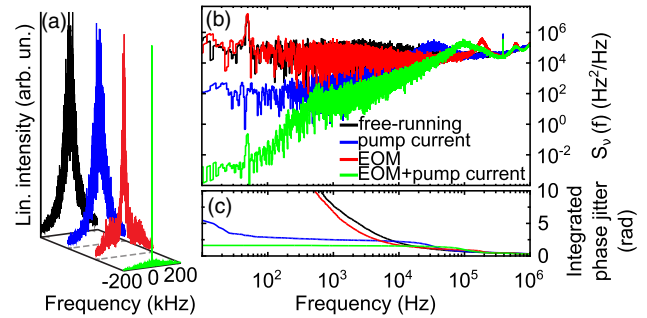


**Fig. 4.** Characterization of the actuator performance for locking of the phase-stable comb on a CW laser: (a) RF spectra, (b) frequency noise, (c) integrated phase jitter. PID settings are constant for all measurements. Color coding: free-running (black), only pump current control (blue), only EOM (red), and a combination of pump current and electro-optic modulator with a final phase jitter of 1.6 rad (green).

of the actuators is illustrated in Fig. 4. The free-running case is depicted with black lines. When only the pump current is controlled (blue spectra), the phase jitter is greatly reduced to 5 rad. At the same time, the comb linewidth slightly increases. This effect is due to the nonlinear feedback inside the cavity leading to amplification of relaxation oscillations that manifest as a maximum in the frequency noise at 34 kHz. When only the EOM is active, the RF spectrum shows significant narrowing, as the noise at frequencies below 100 kHz is efficiently addressed (red spectra). Since the EOM provides a dynamic range of phase shift of 25 rad, the repetition rate may be controlled only for short time intervals. Therefore, the integrated phase jitter is hardly lowered as compared to the free-running case. Both actuators can be adjusted to cooperate perfectly. Controlling the current of the pump diode removes the noise efficiently at low frequencies, while the EOM compensates any timing jitter above 20 kHz. This leads to an even further reduction in the overall phase jitter from 5 to 1.6 rad when integrated from 4 MHz to 1 Hz. We take a closer look at the stabilized performance by analyzing the locked linewidth at the ultimate resolution of our spectrum analyzer. Figure 5 shows the details of the RF spectrum corresponding to the green graphs

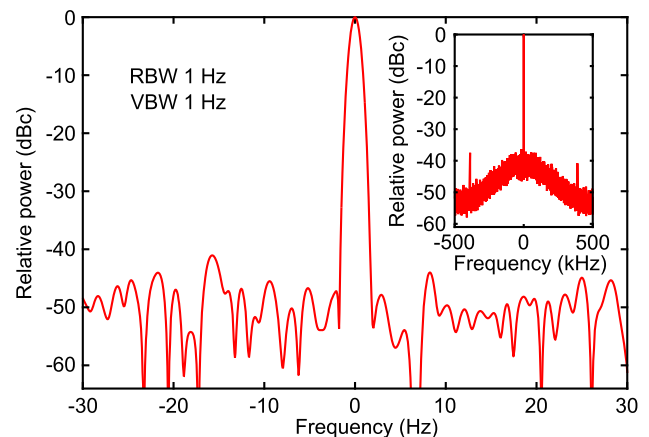


**Fig. 5.** Resolution-limited RF spectrum of an actively narrowed beat between the phase-stable comb and CW reference laser. RBW and video bandwidth (VBW) are set to 1 Hz for both measurements. The span is 60 Hz and 1 MHz (inset). Note the logarithmic scale of both ordinates.

in Fig. 4 on a logarithmic scale over a range of 60 Hz and 1 MHz. The measured linewidth of the beat is instrument-limited and below 1 Hz, while the noise is suppressed over 40 dB.

## 5. DIRECT LOCKING TO AN OPTICAL ATOMIC FREQUENCY STANDARD

Since the repetition rate remains the only parameter in our system that needs active control, absolute locking of this quantity to an optical frequency standard represents the next attractive task we seek to accomplish. For compact applications in harsh environments, atomic absorption lines provided by gas reference cells are a robust, maintenance-free, and cost-effective choice with good fractional stability. We therefore demonstrate direct locking of the repetition rate to a two-photon transition (TPT) in isotopically pure  $^{85}\text{Rb}$ . The TPT is a known candidate for high-stability frequency measurements [34], where a dipole-forbidden transition possesses a natural linewidth of only 660 kHz [35]. It may be excited not only by one but with all combinations of different comb lines, provided they are pairwise two-photon resonant. Nonlinear absorption is therefore greatly enhanced when pumping with a femtosecond comb if it is CEO-stable and symmetric with respect to the TPT frequency. Furthermore, a background-free detection of the absorption is achieved via fluorescent decay of the  $^6\text{P}_{3/2} - ^5\text{S}_{1/2}$  transition at 420 nm. The possibility of spurious detection events is minimized by spectral filtering and near-IR-blind detection. A pulse duration of 110 fs out of the phase-stable erbium-doped fiber amplifier (EDFA 2) with an average power of 630 mW at a repetition rate of 100 MHz allows for efficient second-harmonic generation of the pulse train to a center wavelength of 778 nm. In this process, the brightness of the comb lines is dramatically increased through spectral compression [36]. With lengths of the periodically poled lithium niobate (PPLN) crystals between 1 and 40 mm, a resultant average power of 150 mW is distributed over a spectral bandwidth ranging from 6 nm (corresponding to 5  $\mu\text{W}$  per mode) down to 0.14 nm (power per mode as high as 200  $\mu\text{W}$ ). This feature allows for direct locking of the frequency comb to the  $^5\text{S}_{1/2} - ^5\text{D}_{5/2}$  TPT in  $^{85}\text{Rb}$  [37]. No single-line reference laser is required. We use a 6-nm-broad spectrum centered at a wavelength of 778 nm. This pulse train is dispersed by a grating with 2400 lines/mm. The spectral parts around 776 and 780 nm are then focused from opposite sides into a  $^{85}\text{Rb}$  vapor cell by lenses with focal lengths of  $f = 15$  cm (Fig. 6). Filtering out the central wavelength of 778 nm avoids excitation with two photons propagating in the same direction, thus ensuring Doppler-free operation. Temporal overlap is achieved with a variable delay line (VD). Two-photon absorption is monitored with a photomultiplier tube (PMT) detecting the fluorescence emission at a wavelength of 420 nm. The 240 ns lifetime of this transition [38] enables feedback at a high bandwidth. The spot size of the overlapped excitation beams is 80  $\mu\text{m}$ , and the average power is 30 mW in each branch. To determine the transfer function of this detection scheme, we modulate the current of the pump diode of the oscillator. The photomultiplier tube (PMT) signal gives access to the feedback bandwidth when the position of the comb tooth is varied with respect to the maximum slope of the TPT. The change in the PMT output due to intensity variation is negligible as compared to the induced frequency variation, since both EDFAs are operated in saturation. The results are summarized in Fig. 7(a). A 3 dB roll-off at 70 kHz limited by the bandwidth

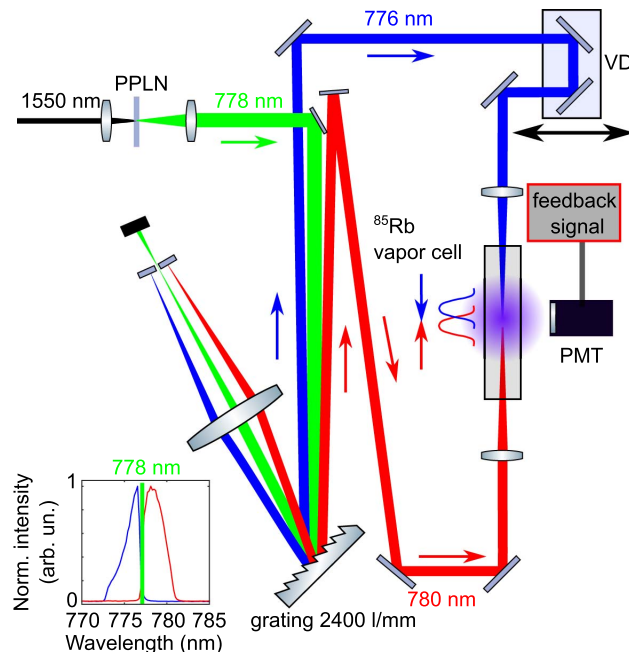


**Fig. 6.** Setup for Doppler-free locking to the  $^5\text{S}_{1/2} - ^5\text{D}_{5/2}$  two-photon optical transition of the  $^{85}\text{Rb}$  atom. The passively phase-stable comb is frequency doubled to a wavelength of 778 nm with a periodically poled lithium niobate crystal (PPLN, length 1 mm, poling period 19.4  $\mu\text{m}$ ) and the beam diameter extended to 1.8 mm ( $1/e^2$ ) prior to the focusing element. The center frequency at 778 nm (green) is blocked, and the beam is spectrally separated in a grating-based pulse shaper. The long (red) and short (blue) wavelength parts (see inset for measured spectra) are then overlapped spatiotemporally in a vapor cell filled with  $^{85}\text{Rb}$ . Fluorescence at a wavelength of 420 nm is emitted after excitation of the two-photon transition and collected with a photomultiplier tube (PMT), providing the error signal for the active locking operation.

of our pump current modulation is measured. To absolutely stabilize the repetition rate, the detected fluorescence is now used as an error signal for a PID controller. The quality of the PMT output is high enough that no modulation, e.g., in a lock-in scheme, is needed. The set point is adjusted to the steepest slope of the TPT, and the pump current is controlled to lock  $f_{\text{rep}}$ . A frequency counter monitors the repetition rate at a gate time of

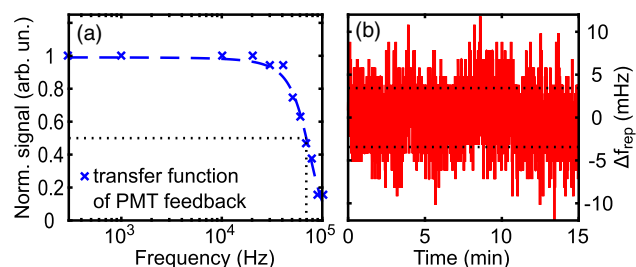


**Fig. 7.** (a) Normalized two-photon fluorescence signal from  $^{85}\text{Rb}$  detected with NIR-blind PMT is depicted as a function of the modulation frequency of the diode pump current. A roll-off bandwidth of 70 kHz is measured. (b) Deviation of the repetition rate ( $\Delta f_{\text{rep}}$ ) from the mean value when locked to the two-photon transition via the diode pump current (gate time of 300 ms). The standard deviation of 3.4 mHz (dotted level) is equivalent to a fractional stability of  $3.4 \times 10^{-11}$  of  $f_{\text{rep}} = 101,382,728.712$  Hz.

300 ms. A typical measurement of the repetition rate acquired over a time interval of 15 min is shown in Fig. 7(b). The standard deviation is 3.4 mHz, corresponding to a fractional stability of  $3.4 \times 10^{-11}$ . Note that the short-time fractional stability of the frequency counter we use is  $2 \times 10^{-11}$  at 1 s, contributing a significant part of the variation in  $f_{\text{rep}}$  we measure.

## 6. CONCLUSION

In summary, we have taken full advantage of several attractive features provided by passive elimination of the carrier-envelope phase slip in a fiber-based frequency comb system via DFG and subsequent re-amplification. To this end, we first analyze the free-running performance of the system. It is found to be dominated by quantum phenomena related to the low pulse energies circulating in our self-starting all-fiber solitonic oscillator. Since only the repetition rate remains as a free parameter of the synthesized comb, we can actively stabilize the entire system without implementing any additional intracavity elements. Controlling the drive current of the pump diode and correcting for minute phase jitter remaining at high frequencies with an EOM outside the cavity enables stabilization to a subhertz linewidth, corresponding to the maximum resolution of our RF analyzer. Doppler-free locking to a two-photon transition (TPT) of  $^{85}\text{Rb}$  is demonstrated without using an intermediate reference. This compact and robust scheme results in a standard deviation of the 100 MHz repetition rate of 3.4 mHz over 15 min. More long-term operation could be achieved by removing the thermal drift of the present setup.

**Funding.** Airbus DS GmbH, Friedrichshafen, Germany European Research Council (ERC) (290876).

**Acknowledgment.** We thank D. Weise, Ch. Jentsch, H.-R. Schulte and U. Johann from Airbus DS GmbH, Friedrichshafen, Germany for their support.

## REFERENCES

- D. J. Jones, S. A. Diddams, J. K. Ranka, A. Stentz, R. S. Windeler, J. L. Hall, and S. T. Cundiff, "Carrier-envelope phase control of femtosecond mode-locked lasers and direct optical frequency synthesis," *Science* **288**, 635–639 (2000).
- T. Udem, R. Holzwarth, and T. W. Hänsch, "Optical frequency metrology," *Nature* **416**, 233–237 (2002).
- S. A. Diddams, "The evolving optical frequency comb [Invited]," *J. Opt. Soc. Am. B* **27**, B51–B62 (2010).
- D. Nicolodi, B. Argence, W. Zhang, R. Le Targat, G. Santarelli, and Y. Le Coq, "Spectral purity transfer between optical wavelengths at the 10-18 level," *Nat. Photonics* **8**, 219–223 (2014).
- N. R. Newbury, "Searching for applications with a fine-tooth comb," *Nat. Photonics* **5**, 186–188 (2011).
- F. Tauser, A. Leitenstorfer, and W. Zinth, "Amplified femtosecond pulses from an Er: fiber system: nonlinear pulse shortening and self-referencing detection of the carrier-envelope phase evolution," *Opt. Express* **11**, 594–600 (2003).
- F.-L. Hong, K. Minoshima, A. Onae, H. Inaba, H. Takada, A. Hirai, H. Matsumoto, T. Sugiura, and M. Yoshida, "Broad-spectrum frequency comb generation and carrier-envelope offset frequency measurement by second-harmonic generation of a mode-locked fiber laser," *Opt. Lett.* **28**, 1516–1518 (2003).
- B. R. Washburn, S. A. Diddams, N. R. Newbury, J. W. Nicholson, M. F. Yan, and C. G. Jorgensen, "Phase-locked, erbium-fiber-laser-based frequency comb in the near infrared," *Opt. Lett.* **29**, 250–252 (2004).
- L. C. Sinclair, I. Coddington, W. C. Swann, G. B. Rieker, A. Hati, K. Iwakuni, and N. R. Newbury, "Operation of an optically coherent frequency comb outside the metrology lab," *Opt. Express* **22**, 6996–7006 (2014).
- D. D. Hudson, K. W. Holman, R. J. Jones, S. T. Cundiff, J. Ye, and D. J. Jones, "Mode-locked fiber laser frequency-controlled with an intracavity electro-optic modulator," *Opt. Lett.* **30**, 2948–2950 (2005).
- S. Koke, C. Grebing, H. Frei, A. Anderson, A. Assion, and G. Steinmeyer, "Direct frequency comb synthesis with arbitrary offset and shot-noise-limited phase noise," *Nat. Photonics* **4**, 462–465 (2010).
- A. Baltuška, T. Fuji, and T. Kobayashi, "Controlling the carrier-envelope phase of ultrashort light pulses with optical parametric amplifiers," *Phys. Rev. Lett.* **88**, 4–7 (2002).
- G. Krauss, D. Fehrenbacher, D. Brida, C. Riek, A. Sell, R. Huber, and A. Leitenstorfer, "All-passive phase locking of a compact Er: fiber laser system," *Opt. Lett.* **36**, 540–542 (2011).
- A. Sell, G. Krauss, R. Scheu, R. Huber, and A. Leitenstorfer, "8-fs pulses from a compact Er: fiber system: quantitative modeling and experimental implementation," *Opt. Express* **17**, 1070–1077 (2009).
- S. Kumkar, G. Krauss, M. Wunram, D. Fehrenbacher, U. Demirbas, D. Brida, and A. Leitenstorfer, "Femtosecond coherent seeding of a broadband Tm: fiber amplifier by an Er: fiber system," *Opt. Lett.* **37**, 554–556 (2012).
- D. Brida, G. Krauss, A. Sell, and A. Leitenstorfer, "Ultrabroadband Er: fiber lasers," *Laser Photon. Rev.* **8**, 409–428 (2014).
- J. Lee, K. Lee, Y.-S. Jang, H. Jang, S. Han, S.-H. Lee, K.-I. Kang, C.-W. Lim, Y.-J. Kim, and S.-W. Kim, "Testing of a femtosecond pulse laser in outer space," *Sci. Rep.* **4**, 05134 (2014).
- A. G. Glenday, C.-H. Li, N. Langellier, G. Chang, L.-J. Chen, G. Furesz, A. A. Zibrov, F. X. Kärtner, D. F. Phillips, D. Sasselov, A. Szentgyorgyi, and R. L. Walsworth, "Operation of a broadband visible-wavelength astro-comb with a high-resolution astrophysical spectrograph," *Optica* **2**, 250–254 (2015).
- M. Wunram, P. Storz, D. Brida, and A. Leitenstorfer, "Ultrastable fiber amplifier delivering 145-fs pulses with 6- $\mu\text{J}$  energy at 10-MHz repetition rate," *Opt. Lett.* **40**, 823–826 (2015).
- T. Nakamura, I. Ito, and Y. Kobayashi, "Offset-free broadband Yb: fiber optical frequency comb for optical clocks," *Opt. Express* **23**, 19376–19381 (2015).
- N. Bucalovic, V. Dolgovskiy, C. Schori, P. Thomann, G. Di Domenico, and S. Schilt, "Experimental validation of a simple approximation to determine the linewidth of a laser from its frequency noise spectrum," *Appl. Opt.* **51**, 4582–4588 (2012).
- M. Takeda, H. Ina, and S. Kobayashi, "Fourier-transform method of fringe-pattern analysis for computer-based topography and interferometry," *J. Opt. Soc. Am.* **72**, 156–160 (1982).
- N. R. Newbury and W. C. Swann, "Low-noise fiber-laser frequency combs (Invited)," *J. Opt. Soc. Am. B* **24**, 1756–1770 (2007).
- D. S. Elliott, R. Roy, and S. J. Smith, "Extracavity laser band-shape and bandwidth modification," *Phys. Rev. A* **26**, 12–18 (1982).
- N. Haverkamp, H. Hundertmark, C. Fallnich, and H. R. Telle, "Frequency stabilization of mode-locked erbium fiber lasers using pump power control," *Appl. Phys. B* **78**, 321–324 (2004).
- J. P. Gordon and H. A. Haus, "Random walk of coherently amplified solitons in optical fiber transmission," *Opt. Lett.* **11**, 665–667 (1986).
- R. Paschotta, "Timing jitter and phase noise of mode-locked fiber lasers," *Opt. Express* **18**, 153–162 (2010).
- H. A. Haus and A. Mecozzi, "Noise of mode-locked lasers," *IEEE J. Quantum Electron.* **29**, 983–996 (1993).
- J. J. McFerran, W. C. Swann, B. R. Washburn, and N. R. Newbury, "Elimination of pump-induced frequency jitter on fiber-laser frequency combs," *Opt. Lett.* **31**, 1997–1999 (2006).
- F. Adler, M. J. Thorpe, and K. C. Cossel, "Cavity-enhanced direct frequency comb spectroscopy: technology and applications," *Annu. Rev. Anal. Chem.* **3**, 175–205 (2010).
- A. Bartels, S. A. Diddams, C. W. Oates, G. Wilpers, J. C. Bergquist, W. H. Oskay, and L. Hollberg, "Femtosecond-laser-based synthesis of ultrastable microwave signals from optical frequency references," *Opt. Lett.* **30**, 667–669 (2005).
- J. Millo, R. Boudot, M. Lours, P. Y. Bourgeois, A. N. Luiten, Y. Le Coq, Y. Kersalé, and G. Santarelli, "Ultra-low-noise microwave extraction from fiber-based optical frequency comb," *Opt. Lett.* **34**, 3707–3709 (2009).

33. J. A. Cox, W. P. Putnam, A. Sell, A. Leitenstorfer, and F. X. Kärtner, "Pulse synthesis in the single-cycle regime from independent mode-locked lasers using attosecond-precision feedback," *Opt. Lett.* **37**, 3579–3581 (2012).
34. T. J. Quinn, "Practical realization of the definition of the metre, including recommended radiations of other optical frequency standards (2001)," *Metrologia* **40**, 103–133 (2003).
35. T. T. Grove, V. Sanchez-Villicana, B. C. Duncan, S. Maleki, and P. L. Gould, "Two-photon two-color diode laser spectroscopy of the Rb  $5D_{5/2}$  state," *Phys. Scr.* **52**, 271–276 (1995).
36. K. Moutzouris, F. Sotier, F. Adler, and A. Leitenstorfer, "Highly efficient second, third and fourth harmonic generation from a two-branch femtosecond erbium fiber source," *Opt. Express* **14**, 1905–1912 (2006).
37. D. Hou, J. Wu, S. Zhang, Q. Ren, Z. Zhang, and J. Zhao, "A stable frequency comb directly referenced to rubidium electromagnetically induced transparency and two-photon transitions," *Appl. Phys. Lett.* **104**, 111104 (2014).
38. D. Sheng, A. Pérez Galván, and L. A. Orozco, "Lifetime measurements of the 5d states of rubidium," *Phys. Rev. A* **78**, 062506 (2008).